Accurate forces in quantum Monte Carlo calculations with nonlocal pseudopotentials

A. Badinski and R. J. Needs
Theory of Condensed Matter Group, Cavendish Laboratory, J. J. Thomson Avenue, Cambridge CB3 0HE, United Kingdom
(Received 27 April 2007; published 18 September 2007)

Calculating accurate forces within variational and diffusion Monte Carlo (VMC and DMC) methods is a very challenging problem. We derive expressions for the contribution to the Hellmann-Feynman force from nonlocal pseudopotentials for use within the VMC and DMC methods. Equilibrium bond lengths and harmonic vibrational frequencies are calculated from the Hellmann-Feynman forces and compared with those obtained from the energies at the Hartree-Fock, VMC, and pure DMC levels. Results for five small molecules show that the equilibrium bond lengths obtained from the force and energy calculations differ by less than 0.007 Å at the DMC level.

DOI: 10.1103/PhysRevE.76.036707 PACS number(s): 02.70.Ss, 31.25.−v, 71.10.−w, 71.15.−m

I. INTRODUCTION

Quantum Monte Carlo (QMC) methods [1] are used to calculate ground-state total energies of many-particle systems. For atoms, molecules, and solids, the calculated energies are comparable to, and often more accurate than, those obtained from density functional theory (DFT) or conventional quantum chemistry methods. To date, QMC calculations have normally used geometries obtained from other theoretical methods or from experiment. It would be more consistent to use geometries calculated within the QMC simulation, which are most conveniently obtained from atomic forces. It has, however, proved difficult to develop accurate and efficient methods for calculating atomic forces within the QMC method.

Let us recall how interatomic forces may be calculated in conventional electronic structure methods. The force on an atom is the negative of the gradient of the energy with respect to the atomic position. The Hellmann-Feynman theorem (HFT) [2,3] states that the gradient of the energy is the expectation value of the gradient of the Hamiltonian; terms involving the gradient of the wave function do not contribute. The HFT holds when the wave function is an exact eigenstate of the Hamiltonian. Within single-particle methods, such as DFT or Hartree-Fock (HF) theory, the orbitals are normally expanded in basis sets, and the HFT holds if the basis set is complete. The HFT also holds when the basis functions are independent of the nuclear positions, as in the case of plane waves. The HFT does not hold when an atom-centered basis set such as a Gaussian is used and the "Pulay" error terms contain gradients of the orbitals with respect to the nuclear positions [4,5].

The role of the HFT within variational Monte Carlo (VMC) calculations is similar to that in conventional electronic structure methods. In VMC one chooses a trial many-body wave function Ψ_T which contains parameters whose optimal values depend on the atomic positions. The energy is evaluated as the expectation value of the Hamiltonian with Ψ_T, and the HFT holds if two conditions apply. First, the values of all variable parameters must be chosen to minimize the energy. Second, the functional form of Ψ_T must be chosen such that it depends only implicitly on the nuclear positions, or, alternatively, the atomic basis centers are considered as variational parameters as well [6]. However, in practice both conditions are generally not satisfied. It is more convenient to choose forms of Ψ_T that have explicit dependence on the nuclear positions. Also, the parameter values are usually obtained by stochastic methods and are therefore subject to statistical noise. In addition, the parameter values are sometimes obtained by minimizing the variance of the energy rather than the energy itself, although one normally assumes that the parameter values are similar. However, as a result of violating these two conditions, the HFT does not in practice hold within the VMC method, and Pulay terms must be included to obtain the correct total derivative of the energy. Evaluating the Pulay terms, in turn, demands the construction, optimization, and evaluation of trial functions for each required gradient.

Some additional issues arise when considering the HFT within the diffusion Monte Carlo (DMC) method. In this method, the imaginary-time Schrödinger equation is used to evolve a set of configurations toward the ground-state distribution. Fermionic symmetry is maintained by the fixed-node approximation [7], in which the nodal surface of the DMC wave function Φ is constrained to equal that of Ψ_T. The DMC algorithm generates the "mixed" distribution $\Psi_T\Phi$. Taking the gradient of the mixed estimator for the fixed-node DMC energy leads to Pulay-like terms, and the estimate of the force is unbiased only when these terms are included. The additional terms include gradients of Φ with respect to the nuclear positions, which cannot be evaluated straightforwardly. Reynolds *et al.* [8,9] replaced these terms by similar ones involving the gradient of Ψ_T, obtaining a scheme which, although approximate, should give good results if Ψ_T is accurate enough. They applied their scheme to the H_2 molecule.

One may also generate the "pure" DMC distribution $\Phi\Phi$ using, for example, the reptation Monte Carlo method [10], the future walking method [11], or the approximate extrapolated estimation method [12]. The HFT force calculated with the pure distribution is not, in general, equal to the negative of the exact DMC energy gradient. If the nodal surface of Ψ_T is approximate, the pure distribution is also approximate and the HFT does not in general hold. Huang *et al.* [13] showed that the gradient of the fixed-node DMC energy evaluated with the pure DMC distribution contains an additional "nodal term" beyond the HFT force, which is zero when the

nodal surface of Ψ_T is exact, and Schautz and Flad [14] gave an explicit expression for this nodal term. Nevertheless, the nodal term is expected to be small in many practical applications, an assumption that can be tested by comparing HFT forces with direct evaluation of the DMC energy at different geometries.

A problem common to the evaluation of forces within both VMC and DMC methods is that the variance of the HFT force is infinite when the bare Coulomb potential is used for the electron-nucleus interaction. This problem was addressed by Assaraf and Caffarel [15,16], who added a term to the HFT force which has zero mean value but greatly reduces the variance of the estimator. It is worth noting that Reynolds *et al.* [9] had included a similar term in their earlier calculation of DMC forces. Alternatively, one can use the filtering method of Chiesa *et al.* [17]. A different route to forces within the QMC method is provided by finite-difference energy calculations [12]. This has been developed within correlated sampling VMC and DMC techniques [18] as well as the reptation Monte Carlo method [19].

The cost of DMC calculations for an all-electron atom of atomic number Z scales roughly as $Z^{5.5}$ [20,21], which makes applications to heavy atoms prohibitively expensive. Pseudopotentials are therefore normally used for heavy atoms, removing the chemically inert core electrons and their rapid spatial variations from the problem. It is advantageous to use pseudopotentials that are smooth at the origin, such as the HF pseudopotentials of Refs. [22,23], which eliminate the problem of the infinite variance of the HFT estimator. Pseudopotentials do, however, introduce an additional complexity, the evaluation of the gradient of the nonlocal pseudopotential operator with respect to the nuclear position. In this paper, we derive the relevant expressions for the gradient of the nonlocal pseudopotential operator.

We investigate the accuracy of the HFT forces for the H_2, LiH, SiH, SiH_4, and GeH molecules within the HF, VMC, and DMC methods. Bond lengths and harmonic vibrational frequencies calculated using the HFT are compared with values obtained from energy calculations. These results are used to demonstrate the validity of our expressions for the nonlocal contributions to the HFT forces, and to investigate the accuracy of the HFT forces in the QMC method.

This paper is organized as follows. In Sec. II we develop the theory of HFT forces in pseudopotential QMC calculations, and sketch the derivation of the expressions for the nonlocal contribution to the HFT forces, which are given in the Appendix. In Sec. III we describe our QMC calculations and in Sec. IV we report tests of the evaluation of our HFT expressions. In Sec. V we present and discuss the molecular bond lengths and vibrational frequencies obtained, and we draw our conclusions in Sec. VI.

II. HFT FORCES IN THE QMC METHOD

We write the valence Hamiltonian as

$$\hat{H} = H_{loc} + \hat{W}, \tag{1}$$

where $\hat{W}$ is the nonlocal pseudopotential operator and H_{loc} comprises the kinetic energy, the Coulomb interaction between the electrons and the local pseudopotential,

$$H_{loc} = -\frac{1}{2}\sum_i \nabla_i^2 + \sum_{i<j}\frac{1}{r_{ij}} + \sum_{i,\alpha} V_{loc}(r_{i\alpha}), \tag{2}$$

where i and j denote electrons, and α labels pseudoions. Unfortunately, it is not straightforward to evaluate the action of $\hat{W}$ on the DMC wave function. In this work we use two different pseudopotential localization schemes. Within the first scheme [24,25], the nonlocal pseudopotential of the Hamiltonian in Eq. (1) is replaced by an effective local potential,

$$\hat{H}_A = H_{loc} + \frac{\hat{W}\Psi_T}{\Psi_T}, \tag{3}$$

where Ψ_T is the trial wave function. In the second localization scheme, recently proposed by Casula [26], the Hamiltonian of Eq. (1) is written in the form

$$\hat{H}_B = H_{loc} + \frac{\hat{W}^+\Psi_T}{\Psi_T} + \hat{W}^-, \tag{4}$$

where the nonlocal pseudopotential operator $\hat{W}^+$ corresponds to all positive matrix elements $\langle \mathbf{R}|\hat{W}|\mathbf{R}'\rangle$, and $\hat{W}^-$ to all negative matrix elements [26]. We will refer to Eq. (3) as the full pseudopotential localization approximation (FPLA) and to Eq. (4) as the semi-PLA (SPLA). Within the SPLA, $\hat{W}^+$ is localized by acting it on Ψ_T, while the action of $\hat{W}^-$ is incorporated into the diffusion process [26], so that localization of $\hat{W}^-$ is not required. Note that the identity $\hat{H}_A\Psi_T = \hat{H}_B\Psi_T$ holds, so that the local energies $\Psi_T^{-1}\hat{H}_A\Psi_T$ and $\Psi_T^{-1}\hat{H}_B\Psi_T$ are identical.

The pure estimate of the Hellmann-Feynman force [2,3] within the FPLA is

$$F_A^{\mathrm{HFT}} = -\frac{\langle\Phi_A|\nabla_{\mathbf{R}}\hat{H}_A|\Phi_A\rangle}{\langle\Phi_A|\Phi_A\rangle} = -\frac{\langle\Phi_A|\nabla_{\mathbf{R}}\sum_{i,\alpha} V_{loc} + \nabla_{\mathbf{R}}(\Psi_T^{-1}\hat{W}\Psi_T)|\Phi_A\rangle}{\langle\Phi_A|\Phi_A\rangle}, \tag{5}$$

where $\nabla_{\mathbf{R}}$ is the gradient with respect to the nuclear coordinates $\mathbf{R}$. The $\hat{W}$ term in Eq. (5) can be written as

$$\nabla_{\mathbf{R}}\left(\frac{\hat{W}\Psi_T}{\Psi_T}\right) = \frac{(\nabla_{\mathbf{R}}\hat{W})\Psi_T}{\Psi_T} + \frac{\hat{W}(\nabla_{\mathbf{R}}\Psi_T)}{\Psi_T} - \frac{(\hat{W}\Psi_T)}{\Psi_T}\frac{(\nabla_{\mathbf{R}}\Psi_T)}{\Psi_T}. \tag{6}$$

The expression equivalent to Eq. (5) within the VMC method is obtained by replacing Φ_A by Ψ_T. The expectation value of the sum of the last two terms in Eq. (6) is zero within the VMC method, but is nonzero within the DMC calculation unless Ψ_T is exact. In practice, the expectation value of the sum of these terms is expected to be small within the DMC method and, because they contain gradients

of the wave function, we classify them as additional Pulay terms. These terms have been neglected in this work and we use

$$F_A^{\mathrm{HFT}} \simeq -\frac{\langle \Phi_A | \nabla_{\mathbf{R}} \sum_{i,\alpha} V_{loc} + \Psi_T^{-1} (\nabla_{\mathbf{R}} \hat{W}) \Psi_T | \Phi_A \rangle}{\langle \Phi_A | \Phi_A \rangle}. \quad (7)$$

The effective local potential within the FPLA can be written as

$$\frac{\hat{W}\Psi_T}{\Psi_T} = \sum_{l,i,\alpha} \frac{2l+1}{4\pi} v_l(r_{i\alpha}) \times \int d\Omega'_{i\alpha} P_l(\Omega'_{i\alpha}) \frac{\Psi(\mathbf{r}_1, \ldots, \mathbf{r}'_i, \ldots, \mathbf{r}_N)}{\Psi(\mathbf{r}_1, \ldots, \mathbf{r}_i, \ldots, \mathbf{r}_N)}, \quad (8)$$

where v_l is a radial pseudopotential for angular momentum l, P_l is a Legendre polynomial, and Ω denotes the corresponding angular variable. The angular integral in Eq. (8) is evaluated by quadrature on the surface of the sphere of radius $r_{i\alpha}$.

We now derive an explicit expression for the contribution of $\hat{W}$ to the HFT force of Eq. (7). To calculate the force on an atom placed at the origin, we consider an infinitesimal displacement $\mathbf{\Delta}=(x,0,0)$ of it, so that the contribution to the x component of the HFT force is given by

$$\left. \frac{d\hat{W}}{dx} \right|_{x=0} \Psi_T(0) = \lim_{x \to 0} \frac{[\hat{W}(x) - \hat{W}(0)]\Psi_T(0)}{x}, \quad (9)$$

where $\Psi_T(0)$ is the trial wave function at zero displacement, i.e., $\mathbf{\Delta}=(0,0,0)$. Consider the effect of the one-electron nonlocal operator $\hat{W}$ on the ith electron at position $\mathbf{r}_i$. From Eq. (8) we can see that, when $\mathbf{\Delta}=(0,0,0)$, the integration is over a sphere of radius $|\mathbf{r}_i|$ centered at the origin. After the displacement it is over a sphere of radius $|\mathbf{r}_i - \mathbf{\Delta}|$ centered at $\mathbf{\Delta}=(x,0,0)$. In practice the integral is approximated by a sum over a set of points on the surface of the integration sphere. Hence, to calculate the gradient in Eq. (9), we need to consider the appropriate transformation of each point of the integration grid so that the original grid points at $r_i \mathbf{u}_k$ are transformed to the points $\mathbf{\Delta} + |\mathbf{r}_i - \mathbf{\Delta}| \mathbf{u}_k$, where k labels the grid points. This transformation is illustrated in two dimensions in Fig. 1.

We can now obtain the required expressions by Taylor-expanding $[\hat{W}(\mathbf{\Delta}) - \hat{W}(0)]\Psi_T(0)$ to first order in $\mathbf{\Delta}$. The resulting expressions for the contribution to the force from angular momentum channels $l=0,1,2,3$ are given in the Appendix. It is noteworthy that the nonlocal HFT force components for the different angular momentum channels depend on the gradient of the wave function with respect to the electron coordinates (but *not* the gradient with respect to the atomic position). Although this dependency may seem surprising at first, it can be interpreted geometrically as arising from the change in the region of the nonlocal integration when an atom is displaced, with the wave function held constant.

The analog of Eq. (5) within the SPLA is

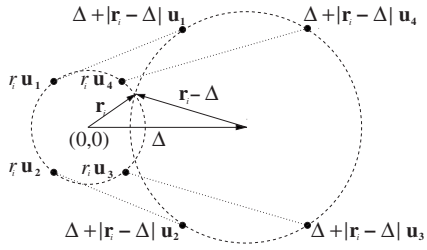

FIG. 1. Illustration of the coordinate transformation of the nonlocal pseudopotential integration grid when displacing an atom centered at the origin (center of the small circle) by the vector $\mathbf{\Delta}$ (center of the large circle). The electron is at $\mathbf{r}_i$. The integration grid at zero displacement consists of four points $r_i \mathbf{u}_1$, etc., which are transformed by the atomic displacement to $\mathbf{\Delta} + |\mathbf{r}_i - \mathbf{\Delta}| \mathbf{u}_1$, etc.

$$F_B^{\mathrm{HFT}} = -\frac{\langle \Phi_B | \nabla_{\mathbf{R}} \hat{H}_B | \Phi_B \rangle}{\langle \Phi_B | \Phi_B \rangle} = -\frac{\langle \Phi_B | \nabla_{\mathbf{R}} \sum_{i,\alpha} V_{loc} + \nabla_{\mathbf{R}} (\Psi_T^{-1} \hat{W}^+ \Psi_T) + \nabla_{\mathbf{R}} \hat{W}^- | \Phi_B \rangle}{\langle \Phi_B | \Phi_B \rangle}. \quad (10)$$

As in the FPLA, we classify the terms in Eq. (10) involving $\nabla_{\mathbf{R}} \Psi_T$ as additional Pulay terms. Since these terms have zero mean within the VMC method, their contribution within the DMC method is assumed to be small and we neglect them. Although the pure estimate in Eq. (5) can be evaluated straightforwardly within the FPLA, a complication arises when using the SPLA, where the nonlocal operator $\nabla_{\mathbf{R}} \hat{W}^-$ acts on the unknown DMC ground-state wave function. We have dealt with this complication by introducing an additional localization approximation when calculating forces within the SPLA,

$$\frac{(\nabla_{\mathbf{R}} \hat{W}^-) \Phi_B}{\Phi_B} \simeq \frac{(\nabla_{\mathbf{R}} \hat{W}^-) \Psi_T}{\Psi_T}. \quad (11)$$

III. QMC CALCULATIONS

We use trial wave functions of the standard single-determinant Slater-Jastrow form. The orbitals forming the Slater determinants are obtained from HF calculations using the CRYSTAL98 [27] and GAMESS-US [28] codes with atomic-centered Gaussian basis sets. For all pseudopotential calculations, the basis set is of sextuple-ζ quality (without f and g functions but with four additional diffuse p and d functions). For the all-electron HF calculations, we use standard basis sets of sextuple-ζ quality from Ref. [29].

We use Jastrow factors consisting of electron-electron, electron-nucleus, and electron-electron-nucleus terms, which are expanded in natural power series. [30] The wave function for H_2 has 87 variable parameters, while those for molecules containing two atomic species have 157. All of the parameters in the Jastrow factors are optimized by first minimizing the variance of the local energy [31] and subsequently by minimizing the energy itself. [32,33]

We use the Dirac-Fock averaged relativistic effective pseudopotentials (AREP) of Refs. [22,23], which can be obtained online. [48] Each pseudopotential contains s, p, and d nonlocal channels. In all calculations, except those reported in Sec. IV, we have chosen the local component of the pseudopotential to be equal to the radial part of the d pseudopotential. The radial components of the pseudopotentials are represented on grids within the QMC calculations, and their derivatives are evaluated numerically using an extended form of Neville's algorithm. [34] All QMC calculations are performed using the CASINO code. [35]

DMC calculations suffer from systematic errors arising from the short-time approximation to the Green's function, which we have carefully investigated for each system studied. We find that the forces calculated with time steps of 0.01, 0.05, and 0.003 a.u. are within one statistical error bar of 0.001 a.u. Therefore, to avoid repeated extrapolation to zero time step for different bond lengths, we use a time step of 0.003 a.u. for all of our DMC calculations and we do not perform any further extrapolation.

As the HFT operator does not commute with the Hamiltonian, the mixed estimator is biased and the pure estimate gives more accurate results. We calculate pure estimates using the future walking method. [11] We also calculate pure expectation values using the extrapolated estimation technique, i.e., $2\times$ (mixed DMC)-VMC. [12] In all our calculations, we find that the extrapolated pure estimates and the future walking pure estimates are in very good agreement. We therefore only report future walking estimates of the pure DMC HFT forces.

Figure 2 summarizes information about the calculations for SiH. The upper graph shows forces evaluated at the Si atom; the lower graph gives the same information for the H atom. As can be seen, the pure DMC estimates are in excellent agreement with the extrapolated estimations for all bond lengths. On the left, the HFT forces are plotted as a function of the future walking projection time, where the mixed DMC estimate corresponds to the future walking one at zero projection time. Although the future walking estimate is exact only for an infinite future walking projection time, we found a projection time of 10 a.u. to be sufficient in our calculations. No significant changes in the estimates were found when using longer projection times. The agreement between the HFT forces obtained from the future walking and extrapolated estimates gives further confidence that our future walking results are well converged.

All of the molecules we have studied consist of H atoms and one heavier atom. It is therefore possible to obtain equilibrium bond lengths and vibrational frequencies from the forces on the H atoms alone. This approach does not, however, directly test the forces on the heavier atoms, where the nonlocality of the pseudopotentials plays a very important role. For all the diatomic molecules, we therefore report bond lengths and vibrational frequencies obtained from using the zero force condition on the H atoms and on the heavier atoms. For SiH_4, the calculated force on the Si atom should be zero by symmetry, and at each level of theory it satisfies this condition to within a statistical error bar of 0.001 a.u. or less. Also, the symmetries of the H_2 and SiH_4 molecules imply that the forces on each H atom should have the same

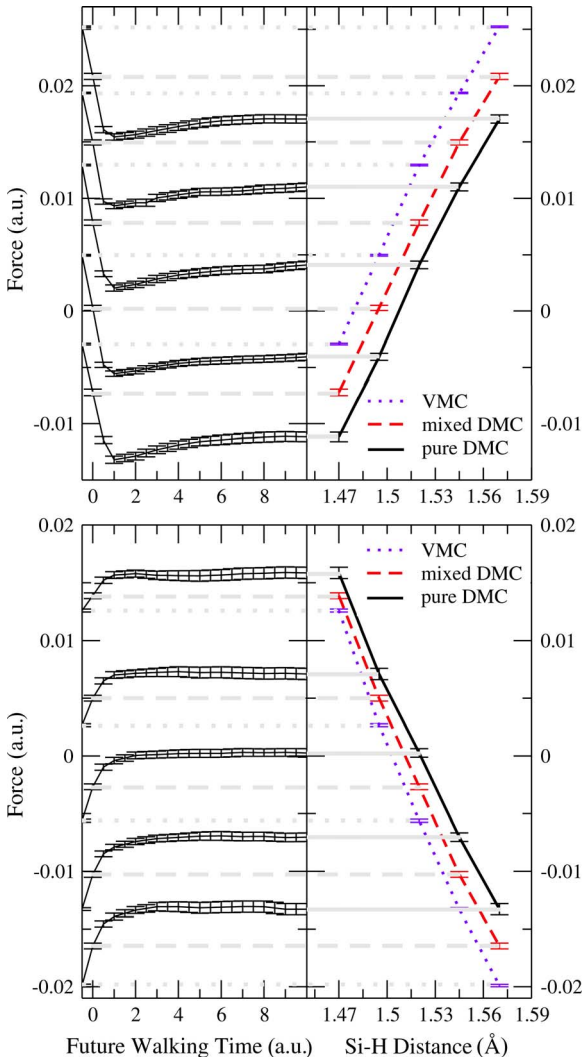

FIG. 2. (Color online) Upper right graph: HFT forces in a.u. on the Si atom in the SiH molecule as calculated within the VMC, mixed DMC, and future walking pure DMC methods for five different bond lengths. Upper left graph: Future walking pure DMC forces plotted against the future walking projection time between 0.5 and 10 a.u. The mixed DMC forces correspond to the zero future walking projection time and the VMC forces are plotted at −0.5 a.u. to guide the reader. Lower graphs: same as the upper ones with the forces now evaluated on the H atom.

magnitude. We found that in each case the forces obey this symmetry to within statistical errors, and we therefore average the symmetry-related components to further reduce the statistical error bars.

To obtain the equilibrium bond lengths, we calculate the HFT forces at 0%, ±1%, and ±2% around the experimental ones, we fit the HFT forces to a quadratic form, and locate the zero-force bond length. In each case the quality of the fit is good and is not significantly changed by using a quartic form. We also calculate the equilibrium bond lengths from the minima in the HF, VMC, and DMC potential energy curves by fitting the energies to cubic polynomials.

TABLE I. Forces (a.u.) on the H and Si atoms of the molecule SiH at the experimental equilibrium bond length. HFVMC, VMC, and pure DMC forces are shown, for estimators where either the s, p, or d angular momentum channel is chosen as local.

	Local channel	F_A^{HFT} on H atom	F_A^{HFT} on Si atom
HFVMC	s	−0.00256330(17995)	0.00355527(10006)
	p	−0.00256327(17995)	0.003467232(9982)
	d	−0.00256325(17995)	0.002518533(9945)
VMC	s	−0.00561230(12888)	0.01277395(16857)
	p	−0.00561228(12888)	0.01286839(16822)
	d	−0.00561227(12887)	0.01296538(16752)
DMC	s	0.00025314(42964)	0.00153481(44006)
	p	0.00025312(42964)	0.00172872(44006)
	d	0.00025310(42964)	0.00193854(44006)

IV. A TEST OF THE EVALUATION OF THE NONLOCAL FORCES

As a test of the correctness of our formulas for the HFT force estimator and our implementation of them, we construct three different estimators by choosing either the s, p, or d angular momentum channels to be local. The three estimates can be obtained from a single HFVMC calculation (the VMC calculation using the determinant part of the wave function only, which should therefore reproduce the HF results within statistical error bars), a VMC calculation including Jastrow factors, and a DMC calculation. The estimates are therefore obtained using correlated sampling, so that the differences between the values obtained by each particular method are much more accurate than the individual values. In Table I we give the total HFT forces at each level of theory for SiH evaluated on both atoms.

For the forces evaluated on the H atom, we find the estimates with different local channels to be almost the same at each level of theory. This is expected because changing the local component of the potential felt by f and higher-angular-momentum wave function components will have very little effect on the H atom. The differences between the forces on the Si atom with different local potentials are considerably larger, but the total forces are small in all cases, which is expected because the calculations are performed at the experimental equilibrium bond length. These results also suggest that contributions by the HFT forces from the angular momenta greater than d are not necessary for these systems.

V. RESULTS AND DISCUSSION

A. Definitions

We define the Pulay errors in quantities such as the bond lengths and vibrational frequencies as the differences between the values obtained from the forces and from the energies,

$$\Delta x_{\mathrm{method}}^{\mathrm{Pulay}} = x_{\mathrm{method}}^{\mathrm{HFT}} - x_{\mathrm{method}}^{E}, \tag{12}$$

where x can either be the bond length a or the vibrational frequency ω, and the method can be HFVMC, VMC, or DMC. In the HFVMC and VMC calculations, the error term Δx arises purely from the Pulay terms that are omitted in our calculations. In the DMC method, this error term has two contributions: first, the Pulay terms, which reduce to a nodal error term within pure DMC [13,14], and second, the terms arising from the pseudopotential localization procedure which involve $\nabla_{\mathbf{R}}\Psi_T$. In the VMC method, such gradient terms have zero mean and therefore do not contribute to the error.

The accuracy of a Jastrow factor can be measured by the percentage of the DMC correlation energy retrieved within the VMC method, i.e.,

$$E_C = \frac{E_{\mathrm{HF}}\text{-}E_{\mathrm{VMC}}}{E_{\mathrm{HF}}\text{-}E_{\mathrm{DMC}}} \times 100\,\%\,, \tag{13}$$

where E_{HF}, E_{VMC}, and E_{DMC} are the HF, VMC, and DMC energies. A perfect Jastrow factor would yield 100% of the DMC correlation energy.

B. Bond lengths

Table II presents equilibrium bond lengths calculated within the HF and HFVMC methods. The excellent agreement between the all-electron and pseudopotential HF bond

TABLE II. Equilibrium bond lengths and Pulay error terms (Å), calculated using the HF and HFVMC methods. For the latter method, results are stated for each atom in the diatomic molecules where (1) indicates the H atom and (2) the heavier atom. The Pulay error $\Delta a_{\mathrm{HFVMC}}^{\mathrm{Pulay}}$ is defined in Eq. (12). All-electron calculations are denoted by (all), while all other theoretical data are for pseudopotential (pp) calculations. The superscripts E and HFT denote bond lengths obtained from the potential energy curve (E) and from the HFT forces (HFT). Experimental values (expt) are taken from Ref. [29] except for GeH which is taken from Ref. [36].

	a_{expt}	$a_{\mathrm{HF(all)}}^{E}$	$a_{\mathrm{HF(pp)}}^{E}$	$a_{\mathrm{HFVMC}}^{\mathrm{HFT}}(1)$	$a_{\mathrm{HFVMC}}^{\mathrm{HFT}}(2)$	$\Delta a_{\mathrm{HFVMC}}^{\mathrm{Pulay}}(1)$	$\Delta a_{\mathrm{HFVMC}}^{\mathrm{Pulay}}(2)$
H_2	0.741	0.7335	0.7334	0.7335(1)		0.0001(1)	
LiH	1.5957	1.6061	1.6031	1.6034(4)	1.6039(4)	0.0003(4)	0.0008(4)
SiH	1.520	1.5131	1.5114	1.5124(7)	1.5122(7)	−0.0010(7)	0.0008(7)
SiH_4	1.480	1.4759	1.4711	1.4720(5)		0.0009(5)	
GeH	1.589	1.5862	1.5858	1.5863(5)	1.5835(5)	0.0005(5)	−0.0023(5)

TABLE III. Equilibrium bond lengths and Pulay error terms (Å), calculated within the VMC and DMC methods. Data for each atom in diatomic molecules are given, where (1) indicates the H atom and (2) the heavier atom. The Pulay errors $\Delta a^{\mathrm{Pulay}}_{\mathrm{VMC}}$ and $\Delta a^{\mathrm{Pulay}}_{\mathrm{DMC}}$ are defined in Eq. (12). The superscripts E and HFT denote bond lengths obtained from the potential energy curve (E) and from the HFT forces (HFT). Experimental values (expt) are taken from Ref. [29], except for GeH which is from Ref. [36].

	a_{expt}	a^{E}_{VMC}	$a^{\mathrm{HFT}}_{\mathrm{VMC}}(1)$	$a^{\mathrm{HFT}}_{\mathrm{VMC}}(2)$	$\Delta a^{\mathrm{Pulay}}_{\mathrm{VMC}}(1)$	$\Delta a^{\mathrm{Pulay}}_{\mathrm{VMC}}(2)$	a^{E}_{DMC}	$a^{\mathrm{HFT}}_{\mathrm{DMC}}(1)$	$a^{\mathrm{HFT}}_{\mathrm{DMC}}(2)$	$\Delta a^{\mathrm{Pulay}}_{\mathrm{DMC}}(1)$	$\Delta a^{\mathrm{Pulay}}_{\mathrm{DMC}}(2)$
H_2	0.741	0.7394(2)	0.7332(1)		−0.0062(2)		0.7413(2)	0.7412(1)		−0.0001(2)	
LiH	1.5957	1.5952(4)	1.6063(8)	1.5911(8)	0.0111(9)	−0.0041(9)	1.6000(3)	1.5995(8)	1.5970(12)	−0.0005(8)	−0.0030(12)
SiH	1.520	1.5169(3)	1.5029(3)	1.4784(4)	−0.0140(4)	−0.0385(5)	1.5173(8)	1.5188(12)	1.5111(17)	0.0015(14)	−0.0062(19)
SiH_4	1.480	1.4736(7)	1.4649(4)		−0.0087(8)		1.4739(5)	1.4727(5)		−0.0012(7)	
GeH	1.589	1.5973(4)	1.5774(3)	1.5620(3)	−0.0199(5)	−0.0353(5)	1.6030(7)	1.6001(14)	1.5956(16)	−0.0029(16)	−0.0074(17)

lengths, $a^{E}_{\mathrm{HF(all)}}$ and $a^{E}_{\mathrm{HF(pp)}}$, indicates the high quality of the pseudopotentials [22,23]. At the HFVMC level, the HFT holds if the basis set is complete. In our calculations, the bond lengths derived from the energies, $a^{E}_{\mathrm{HF(pp)}}$, and the HFT estimators evaluated on each atom, $a^{\mathrm{HFT}}_{\mathrm{HFVMC}}(1)$ and $a^{\mathrm{HFT}}_{\mathrm{HFVMC}}(2)$, agree within twice the statistical error of around 0.0005 Å, with the exception of GeH, where the deviation in the bond length derived from the energies and HFT forces on the Ge atom is $\Delta a^{\mathrm{Pulay}}_{\mathrm{HFT}}=-0.0023(5)$ Å. This high level of agreement provides further evidence for the correctness of our nonlocal force formulas and their implementation. The small differences between the bond lengths calculated from the HFVMC energies and forces arises from the neglected Pulay forces. The small size of the Pulay forces suggests that the Gaussian basis sets are very nearly complete for our molecules, with the exception of the Ge atom in GeH, where the basis set quality is slightly inferior. A small contribution to these differences might also arise from the use of Gaussian parametrizations of the pseudopotentials in our HF calculations as opposed to the grid representations in the QMC calculations.

Table III presents equilibrium bond lengths calculated within the VMC and DMC methods. At the VMC level, adding a Jastrow factor generally does not improve upon the equilibrium bond lengths obtained from HF forces. Our Jastrow factors retrieve well over 90% of the DMC correlation energy E_{C} in Table IV, which would normally be taken to imply that the Jastrow factors are of high quality, but it appears that even higher quality is necessary to obtain accurate forces within the VMC method. We find a clear correlation between the VMC Pulay errors in Table III and the quality of the wave function as measured by the percentages of the DMC correlation energies retrieved as stated in Table IV.

TABLE IV. Total energies (a.u.) within the HF, VMC, and DMC methods at the equilibrium bond lengths given by the minimum in the DMC energy. E_{C} is the percentage of the DMC correlation energy retrieved at the VMC level and is defined in Eq. (13) (its error bars are smaller than the last stated digit).

	E_{HF} (a.u.)	E_{VMC} (a.u.)	E_{DMC} (a.u.)	E_{C} (%)
H_2	−1.13368	−1.173910(5)	−1.17439(1)	98.8
LiH	−0.75060	−0.78780(1)	−0.78811(0)	99.2
SiH	−4.26236	−4.369050(6)	−4.37698(2)	93.1
SiH_4	−6.08890	−6.27142(3)	−6.27906(5)	96.0
GeH	−4.24388	−4.343760(6)	−4.35144(3)	92.9

The DMC results reported in Table III were obtained with the FPLA. In each case, we find that the bond lengths obtained from the forces on the H atoms agree very well with those from the energies. This is reflected in the DMC Pulay terms $\Delta a^{\mathrm{Pulay}}_{\mathrm{DMC}}(1)$ listed in Table III, which are smaller than two statistical error bars. The Pulay terms are largest in GeH, where $\Delta a^{\mathrm{Pulay}}_{\mathrm{DMC}}(1)=0.0029(16)$ Å. The bond lengths obtained from the forces on the heavier atoms are in slightly poorer agreement with the energy data than for the forces on the H atoms, and the corresponding Pulay errors are equal to or smaller than four times their statistical error bars. The largest deviation is found for GeH with $\Delta a^{\mathrm{Pulay}}_{\mathrm{DMC}}(2)=-0.0074(17)$ Å and the smallest for LiH with $\Delta^{\mathrm{Pulay}}_{\mathrm{DMC}}(2)=-0.0030(12)$ Å. Our data therefore suggest that the neglected gradient and nodal terms in our DMC HFT estimates must be very small for the lighter atoms (H and Li), where the wave functions can be assumed to be very accurate. For the heavier atoms (Si and Ge), these neglected terms are larger and lead to small changes in the DMC force estimates and bond lengths. This is understandable since the quality of Ψ_T is lower for the molecules with heavier atoms, as shown by the data in Table IV. It is certainly possible to calculate the Pulay forces corresponding to the neglected $\nabla_{\mathbf{R}}\Psi_T$ terms in Eq. (6), although the nodal term [13,14] would still be neglected.

The differences between the DMC bond lengths (from either the energies or the forces evaluated on either the H or heavier atoms) and experiment are on the whole somewhat larger than the differences between the bond lengths from the DMC energies and forces. The largest differences are found for GeH with 0.0111(14) Å and SiH_4 with 0.0089(17) Å. In the previous paragraph, we concluded that the neglected nodal and gradient terms of the DMC HFT estimator are small for H and Li because the bond lengths from the DMC energies and forces on the H and Li atoms agree. The deviations of these bond lengths from experiment must largely come from a combination of the fixed-node approximation, the FPLA scheme, which slightly alters the pure DMC ground state distribution, and the pseudopotentials. It is certainly possible to reduce the fixed-node error by using more accurate wave function forms, such as multideterminant [37], pairing [38,39], and/or backflow wave functions [40,41]. Unfortunately, developing more accurate pseudopotentials for use in QMC calculations is a difficult task, but including core

TABLE V. Harmonic vibrational frequencies and Pulay error terms (cm^{-1}) calculated using the HF and HFVMC methods. All abbreviations used in this table as well as references to experimental data are the same as in Table II.

	ω_{expt}	$\omega^{E}_{HF(all)}$	$\omega^{E}_{HF(pp)}$	$\omega^{HFT}_{HFVMC}(1)$	$\omega^{HFT}_{HFVMC}(2)$	$\Delta\omega^{Pulay}_{HFVMC}(1)$	$\Delta\omega^{Pulay}_{HFVMC}(2)$
H_2	4401	4580	4621	4608(24)		−13(24)	
LiH	1406	1488	1419	1425(11)	1424(10)	6(11)	5(11)
SiH	2042	2132	2130	2142(14)	2131(13)	12(14)	1(13)
SiH_4	2187	2336	2340	2370(21)		30(21)	
GeH	1908±35	1986	1979	1966(13)	1988(12)	−13(13)	9(12)

polarization potentials [42–44] on the Li, Si, and Ge atoms might improve the results.

C. Vibrational frequencies

Tables V and VI present harmonic vibrational frequencies obtained from the forces and energies calculated within the HF, HFVMC, VMC, and DMC methods. Our conclusions are similar to those in the discussion of bond lengths. At the HFVMC level, the frequencies obtained from the forces and energies agree within or close to one standard error (see Table V). This is further evidence that the basis sets are of high quality. The harmonic frequencies for the molecules containing Si and Ge atoms are not improved by introducing correlation at the VMC level. The DMC harmonic frequencies are significantly more accurate than the HF and VMC ones. The frequencies obtained from the DMC forces and energies agree within one standard deviation of around 40 cm^{-1}, with the exception of SiH_4, where the difference is $\Delta\omega^{Pulay}_{VMC}(1)=67(43)$ cm^{-1}. We mentioned earlier that the bond lengths obtained from the DMC forces and energies are within four standard errors, but the vibrational frequencies agree within one standard error.

D. Comparison of the FPLA and SPLA schemes

Here we compare the performance of the FPLA and SPLA for SiH and GeH. Although the local energies within the FPLA and SPLA are the same, the schemes generate slightly different ground-state wave functions, and therefore the bond lengths and frequencies from the FPLA and SPLA can differ. In addition, we make slightly different approximations when calculating the forces. The data for the equilibrium bond lengths and vibrational frequencies in Table VII show that the differences obtained within the FPLA and SPLA schemes are fairly small.

E. Comparison of DMC results with other methods

Here we briefly compare our DMC results with those obtained from Moller Plesset (MP2) and coupled cluster (CC) quantum chemistry methods, and Perdew-Burke-Ernzerhof (PBE) DFT, using standard basis sets. Table VIII shows deviations of the bond lengths derived from our pseudopotential DMC HFT force calculations and various all-electron reference calculations from experimental data. The average deviation over all bond lengths is 0.0051(4) Å for our DMC results (where the average is over all bond lengths calculated from forces on the H and heavier atoms), 0.0225 Å for PBE DFT, 0.0025 Å for MP2, and 0.0056 Å for CC methods. Table IX reports similar data for vibrational frequencies. The average deviations from the experimental frequencies are 26(10) cm^{-1} for our DMC results (where the average is over all frequencies calculated from forces on the H and heavier atoms), 57 cm^{-1} for PBE DFT, 79 cm^{-1} for MP2, and 19 cm^{-1} for CC calculations. These comparisons show that our (pseudopotential) DMC bond lengths and vibrational frequencies are at least comparable with those obtained from standard all-electron reference calculations.

For completeness, we summarize results of previous DMC calculations of forces for small molecules and the equilibrium bond lengths obtained. As analytic QMC forces have not previously been calculated with pseudopotentials, we compare with recent all-electron studies. Assaraf and Caffarel [16] calculated HFT forces using a variance reduction scheme, which requires the evaluation of the derivative of Ψ_T and extrapolated estimation to approximate the pure DMC distribution. They report bond lengths for H_2, LiH, and

TABLE VI. Harmonic vibrational frequencies and Pulay error terms (cm^{-1}) calculated using the VMC and DMC methods. All abbreviations used in this table as well as references for experimental data are the same as in Table II.

	ω_{expt}	ω^{E}_{VMC}	$\omega^{HFT}_{VMC}(1)$	$\omega^{HFT}_{VMC}(2)$	$\Delta\omega^{Pulay}_{VMC}(1)$	$\Delta\omega^{Pulay}_{VMC}(2)$	ω^{E}_{DMC}	$\omega^{HFT}_{DMC}(1)$	$\omega^{HFT}_{DMC}(2)$	$\Delta\omega^{Pulay}_{DMC}(1)$	$\Delta\omega^{Pulay}_{DMC}(2)$
H_2	4401	4394(48)	4478(25)		84(54)		4379(30)	4434(35)		55(46)	
LiH	1406	1416(15)	1392(13)	1352(12)	−24(20)	−64(19)	1395(20)	1424(24)	1398(22)	29(31)	3(31)
SiH	2042	2130(15)	2241(9)	2208(11)	111(17)	78(19)	2077(34)	2034(25)	2055(26)	−43(42)	−22(43)
SiH_4	2187	2166(33)	2405(26)		239(42)		2193(27)	2260(33)		67(43)	
GeH	1908±35	1834(11)	2128(50)	2089(52)	294(51)	255(53)	1922(31)	1938(25)	1935(26)	16(39)	13(40)

TABLE VII. Equilibrium bond lengths (Å), vibrational frequencies (cm^{-1}), and their corresponding Pulay error terms calculated with the DMC method for SiH and GeH. Two different localization methods (FPLA and SPLA) are used as indicated in the second column. All other abbreviations used in this table as well as references for experimental data are the same as in Table II.

	Method	a_{expt}	a^{E}_{DMC}	$a^{HFT}_{DMC}(1)$	$a^{HFT}_{DMC}(2)$	$\Delta a^{Pulay}_{DMC}(1)$	$\Delta a^{Pulay}_{DMC}(2)$
SiH	FPLA	1.520	1.5173(8)	1.5188(12)	1.5111(17)	0.0015(14)	−0.0062(19)
	SPLA	1.520	1.5206(9)	1.5190(12)	1.5131(18)	−0.0016(15)	−0.0075(20)
GeH	FPLA	1.589	1.6030(7)	1.6001(14)	1.5956(16)	−0.0029(16)	−0.0074(17)
	SPLA	1.589	1.5968(7)	1.5986(15)	1.5898(17)	0.0018(18)	−0.0070(18)
	Method	ω_{expt}	ω^{E}_{DMC}	$\omega^{HFT}_{DMC}(1)$	$\omega^{HFT}_{DMC}(2)$	$\Delta\omega^{Pulay}_{DMC}(1)$	$\Delta\omega^{Pulay}_{DMC}(2)$
SiH	FPLA	2042	2077(34)	2034(25)	2055(26)	−43(42)	−22(43)
	SPLA	2042	2012(27)	2039(28)	2065(29)	27(39)	53(40)
GeH	FPLA	1908±35	1922(31)	1938(25)	1935(26)	16(39)	13(40)
	SPLA	1908±35	1993(30)	1944(32)	1933(33)	−49(44)	−60(45)

Li_2 with an average deviation from the experimental bond lengths of 0.007(6) Å. Two other studies combine this variance reduction approach with an energy minimization scheme for optimizing Ψ_T and include the evaluation of Pulay terms: Casalegno *et al.* [6] obtain bond lengths from forces with mixed DMC distributions for H_2 and LiH with deviations from the experimental values of 0.001(1) and 0.005(3) Å, respectively. Using the same method, Lee *et al.* [47] present bond lengths for eight diatomic molecules with an average deviation from experiment of 0.0096(2) Å. Chiesa *et al.* [17] calculate pure estimates of the HFT forces on the H atoms for six molecules using a filtering technique, obtaining an average deviation from the experimental results of 0.0021(9) Å.

TABLE VIII. Equilibrium bond lengths (Å) obtained from pseudopotential DMC forces on the H atoms using the FPLA scheme and various all-electron reference methods. The calculated data are given as deviations from the experimental bond lengths. The PBE results are obtained using the augmented correlation consistent polarized valence triple-ζ (aug-cc-pVTZ) basis set [45]. The MP2 results are obtained using the cc-pVTZ basis set, except for LiH, where the 6-311G** basis set is used [29]. The coupled cluster (CC) results are obtained with the cc-pVTZ basis and the CC single, double and triple excitation (CCSD(T)) method [29], except for LiH, where the CCD method is used with a basis set of a quality better than sextuple-ζ [46]. All experimental values are taken from Ref. [29], except for GeH which is from Ref. [36].

	a_{expt}	Δa_{DMC}	Δa_{PBE}	Δa_{MP2}	Δa_{CC}
H_2	0.741	0.0002(1)	0.010	−0.0040	0.0016
LiH	1.5957	0.0038(8)	0.0103	0.0030	0.0002
SiH	1.52	−0.0012(12)	0.0419	0.0002	0.0086
SiH_4	1.480	−0.0073(6)	0.0277	−0.0026	0.0026
GeH	1.589	0.0111(14)			0.0149

VI. CONCLUSIONS

We reported expressions for the contribution to the Hellmann-Feynman force resulting from using nonlocal pseudopotentials in variational and diffusion Monte Carlo calculations. The expressions for the components of the HFT force arising from the nonlocal pseudopotential involve the gradients of the trial wave function with respect to the electron positions.

The HFT does not hold exactly in our methods because we use approximate wave functions. The HFT forces on the atoms of a molecule do not then sum to zero, but their sum goes to zero as the trial nodal surface becomes exact. The DMC energies and HFT forces would be consistent if the terms from the full pseudopotential localization approximation involving $\nabla_{\mathbf{R}}\Psi_T$ were included in Eq. (6), apart from the neglect of the nodal term. We could in principle evaluate the expectation values of these gradient terms but have neglected them in our work. As the expectation values of these terms within the VMC method is zero, and we have obtained very

TABLE IX. Harmonic vibrational frequencies (cm^{-1}) obtained from our pseudopotential DMC HFT force calculations at the H atoms using the FPLA scheme and various all-electron reference methods. The calculated data are given as deviations from the experimental frequencies. The basis sets and references are the same as in Table VIII, with the exception of the PBE frequencies, which are obtained with the cc-pVTZ basis, and are obtained from Ref. [29].

	ω_{expt}	$\Delta\omega_{DMC}$	$\Delta\omega_{PBE}$	$\Delta\omega_{MP2}$	$\Delta\omega_{CC}$
H_2	4401	33(35)	−84	125	9
LiH	1406	−18(24)	−32	35	−2
SiH	2042	−8(25)	87	51	−10
SiH_4	2187	73(33)	−27	109	64
GeH	1908±35	30(25)			−10

good results without them, we conclude that they are small in our calculations.

We calculated bond lengths and harmonic vibrational frequencies from the HFT forces for five small molecules, using single-determinant Slater-Jastrow trial wave functions and VMC and DMC methods. The DMC HFT forces were calculated using future walking pure estimates. We investigated both the FPLA and SPLA schemes for the nonlocal pseudopotential operator and have obtained similar results with them. The equilibrium bond lengths for five small molecules obtained from the force and energy calculations at the DMC level differ by less than 0.003 Å for the forces calculated on the H atoms, and by less than 0.007 Å for the forces on the heavier atoms. The harmonic vibrational frequencies obtained from the DMC forces are in very good agreement with experiment.

Our expressions for the nonlocal forces can be used straightforwardly in systems with periodic boundary conditions. They can also be used in conjunction with other methods for improving DMC forces, such as schemes to reduce the variance of the HFT estimator [15,16], adding Pulay terms [6], or using better trial wave function forms.

ACKNOWLEDGMENTS

We are grateful to Dr. John Trail and Professor Lubos Mitas for helpful discussions. This work was supported by the Engineering and Physical Sciences Research Council of the United Kingdom. Computing resources were provided by the University of Cambridge High Performance Computing Service (HPCS).

APPENDIX: EXPRESSIONS FOR NONLOCAL FORCES

Here we give the expressions for the nonlocal contributions to the Hellmann-Feynman forces for the first four angular momenta $l=0,1,2,3$. These expressions give the x components of the HFT forces; the other components are obtained by replacing x by y or z. $\boldsymbol{\xi}$ denotes a dummy variable for an electron position, $\mathbf{u}_k$ is a unit vector in the direction of the kth point of the nonlocal integration grid (see Fig. 1), and $\mathbf{e}_x$ is the unit vector in the x direction.

$$F^{\mathrm{HFT}}_{x,l=0} = \frac{1}{4\pi}\sum_k \left[v_0(r) \frac{\nabla_{\boldsymbol{\xi}} \Psi\,(\mathbf{r}_1,\ldots,\boldsymbol{\xi},\ldots,\mathbf{r}_N)|_{\boldsymbol{\xi}=r_i\mathbf{u}_\mathbf{k}}}{\Psi(\mathbf{r}_1,\ldots,\mathbf{r}_i,\ldots,\mathbf{r}_N)} \cdot \left(\mathbf{e}_x - \frac{r_{i,x}}{r}\mathbf{u}_k\right) - \frac{r_{i,x}}{r_i} \left.\frac{dv_0(\xi)}{d\xi}\right|_{\xi=r_i} \frac{\Psi(\mathbf{r}_1,\ldots,r_i\mathbf{u}_k,\ldots,\mathbf{r}_N)}{\Psi(\mathbf{r}_1,\ldots,\mathbf{r}_i,\ldots,\mathbf{r}_N)} \right],$$

$$F^{\mathrm{HFT}}_{x,l=1} = \frac{3}{4\pi}\sum_k \left\{ \left[-v_1(r_i)\mathbf{e}_x \cdot \frac{\mathbf{u}_k}{r_i} + v_1(r_i)\left(\mathbf{r}_i\cdot\mathbf{u}_k \frac{r_{i,x}}{r_i^3}\right) - \frac{r_{i,x}}{r_i} \left.\frac{dv_1(\xi)}{d\xi}\right|_{\xi=r_i} \frac{\mathbf{r}_i\cdot\mathbf{u}_k}{r_i} \right] \frac{\Psi(\mathbf{r}_1,\ldots,r_i\mathbf{u}_k,\ldots,\mathbf{r}_N)}{\Psi(\mathbf{r}_1,\ldots,\mathbf{r}_i,\ldots,\mathbf{r}_N)} \right.$$
$$\left. + v_1(r_i)\frac{\mathbf{r}_i\cdot\mathbf{u}_k}{r_i} \frac{\nabla_y \Psi\,(\mathbf{r}_1,\ldots,\boldsymbol{\xi},\ldots,\mathbf{r}_N)|_{\boldsymbol{\xi}=r_i\mathbf{u}_k}}{\Psi(\mathbf{r}_1,\ldots,\mathbf{r}_i,\ldots,\mathbf{r}_N)} \cdot \left(\mathbf{e}_x - \frac{r_{i,x}}{r_i}\mathbf{u}_k\right) \right\},$$

$$F^{\mathrm{HFT}}_{x,l=2} = \frac{5}{4\pi}\sum_k \left[v_2(r_i) \frac{\Psi(\mathbf{r}_1,\ldots,r_i\mathbf{u}_k,\ldots,\mathbf{r}_N)}{\Psi(\mathbf{r}_1,\ldots,\mathbf{r}_i,\ldots,\mathbf{r}_N)} \left(-3\frac{(\mathbf{r}_i\cdot\mathbf{u}_k)}{r_i^2}\mathbf{u}_k + 3\frac{(\mathbf{r}_i\cdot\mathbf{u}_k)^2}{r_i^2}\frac{r_{i,x}}{r_i^2} \right) \right.$$
$$- \left.\frac{dv_2(\xi)}{d\xi}\right|_{\xi=r_i} \frac{\mathbf{r}_i}{r_i} \frac{\Psi(\mathbf{r}_1,\ldots,r_i\mathbf{u}_k,\ldots,\mathbf{r}_N)}{\Psi(\mathbf{r}_1,\ldots,\mathbf{r}_i,\ldots,\mathbf{r}_N)} \left(\frac{3}{2}\frac{(\mathbf{r}_i\cdot\mathbf{u}_k)^2}{r_i^2} - \frac{1}{2} \right)$$
$$\left. + v_2(r_i) \frac{\nabla_{\boldsymbol{\xi}} \Psi\,(\mathbf{r}_1,\ldots,\boldsymbol{\xi},\ldots,\mathbf{r}_N)|_{\boldsymbol{\xi}=r_i\mathbf{u}_k}}{\Psi(\mathbf{r}_1,\ldots,\mathbf{r}_i,\ldots,\mathbf{r}_N)} \cdot \left(\mathbf{e}_x - \frac{r_{i,x}}{r_i}\mathbf{u}_k\right) \left(\frac{3}{2}\frac{(\mathbf{r}_i\cdot\mathbf{u}_k)^2}{r_i^2} - \frac{1}{2} \right) \right],$$

$$F^{\mathrm{HFT}}_{x,l=3} = \frac{7}{4\pi}\sum_k \left\{ \left[v_3(r_i) \left(\frac{5}{r_i^3}(\mathbf{r}_i\cdot\mathbf{u}_k)^3 \frac{r_{i,x}}{r_i^2} - \frac{5}{r_i^3}(\mathbf{r}_i\cdot\mathbf{u}_k)^2 \mathbf{u}_{k,x} + \frac{3}{2r_i}\mathbf{u}_{k,x} - \frac{3}{2r_i}\mathbf{r}_i\cdot\mathbf{u}_k \frac{r_{i,x}}{r_i^2} \right) + \left.\frac{dv_3(\xi)}{d\xi}\right|_{\xi=r_i} \left(\frac{r_{i,x}}{r_i}\frac{3}{2r_i}(\mathbf{r}_i\cdot\mathbf{u}_k) \right.\right.\right.$$
$$\left.\left.\left. - \frac{5}{2r_i^3}(\mathbf{r}_i\cdot\mathbf{u}_k)^3 \right) \right] \frac{\Psi(\mathbf{r}_1,\ldots,r_i\mathbf{u}_k,\ldots,\mathbf{r}_N)}{\Psi(\mathbf{r}_1,\ldots,\mathbf{r}_i,\ldots,\mathbf{r}_N)} + v_3(r_i) \frac{\nabla_{\boldsymbol{\xi}} \Psi\,(\mathbf{r}_1,\ldots,\boldsymbol{\xi},\ldots,\mathbf{r}_N)|_{\boldsymbol{\xi}=r_i\mathbf{u}_k}}{\Psi(\mathbf{r}_1,\ldots,\mathbf{r}_i,\ldots,\mathbf{r}_N)} \cdot \left(\mathbf{e}_x - \frac{r_{i,x}}{r_i}\mathbf{u}_k\right) \left(\frac{5}{2r_i^3}(\mathbf{r}_i\cdot\mathbf{u}_k)^3 \right.\right.$$
$$\left.\left. - \frac{3}{2r_i}(\mathbf{r}_i\cdot\mathbf{u}_k) \right) \right\}.$$

[1] W. M. C. Foulkes, L. Mitas, R. J. Needs, and G. Rajagopal, Rev. Mod. Phys. **73**, 33 (2001).
[2] H. Hellmann, *Einführung in die Quantenchemie* (Franz Deuticke, Vienna, 1937).
[3] R. P. Feynman, Phys. Rev. **56**, 340 (1939).
[4] P. Pulay, Mol. Phys. **17**, 197 (1969).
[5] M. Scheffler, J. P. Vigneron, and G. B. Bachelet, Phys. Rev. B **31**, 6541 (1985).
[6] M. Casalegno, M. Mella, and A. M. Rappe, J. Chem. Phys. **118**, 7193 (2003).
[7] J. B. Anderson, J. Chem. Phys. **65**, 4121 (1976).
[8] P. J. Reynolds, R. N. Barnett, B. L. Hammond, and W. A. Lester, Jr., J. Stat. Phys. **43**, 1017 (1986).
[9] P. J. Reynolds, R. N. Barnett, B. L. Hammond, R. M. Grimes, and W. A. Lester, Jr., Int. J. Quantum Chem. **29**, 589 (1986).
[10] S. Baroni and S. Moroni, Phys. Rev. Lett. **82**, 4745 (1999).
[11] R. N. Barnett, P. J. Reynolds, and W. A. Lester, Jr., J. Comput. Phys. **96**, 258 (1991).
[12] D. M. Ceperley and M. H. Kalos, *Monte Carlo Methods in Statistical Physics*, edited by K. Binder (Springer-Verlag, Berlin, 1979).
[13] K. C. Huang, R. J. Needs, and G. Rajagopal, J. Chem. Phys. **112**, 4419 (2000).
[14] F. Schautz and H.-J. Flad, J. Chem. Phys. **112**, 4421 (2000).
[15] R. Assaraf and M. Caffarel, J. Chem. Phys. **113**, 4028 (2000).
[16] R. Assaraf and M. Caffarel, J. Chem. Phys. **119**, 10536 (2003).
[17] S. Chiesa, D. M. Ceperley, and S. Zhang, Phys. Rev. Lett. **94**, 036404 (2005).
[18] C. Filippi and C. J. Umrigar, Phys. Rev. B **61**, R16291 (2000).
[19] C. Pierleoni and D. M. Ceperley, ChemPhysChem **6**, 1872 (2005).
[20] D. M. Ceperley, J. Stat. Phys. **43**, 815 (1986).
[21] A. Ma, N. D. Drummond, M. D. Towler, and R. J. Needs, Phys. Rev. E **71**, 066704 (2005).
[22] J. R. Trail and R. J. Needs, J. Chem. Phys. **122**, 014112 (2005).
[23] J. R. Trail and R. J. Needs, J. Chem. Phys. **122**, 174109 (2005).
[24] M. M. Hurley and P. A. Christiansen, J. Chem. Phys. **86**, 1069 (1986).
[25] L. Mitas, E. L. Shirley, and D. M. Ceperley, J. Chem. Phys. **95**, 3467 (1991).
[26] M. Casula, Phys. Rev. B **74**, 161102(R) (2006).
[27] V. R. Saunders, R. Dovesi, C. Roetti, M. Causa, N. M. Harrison, R. Orlando, and C. M. Zicovich-Wilson, computer code CRYSTAL98 (University di Torino, Torino, 1998).
[28] M. W. Schmidt, K. K. Baldridge, and J. A. Boatz, J. Comput. Chem. **14**, 1347 (1993).
[29] National Institute of Standards and Technology, http://www.nist.gov
[30] N. D. Drummond, M. D. Towler, and R. J. Needs, Phys. Rev. B **70**, 235119 (2004).
[31] N. D. Drummond and R. J. Needs, Phys. Rev. B **72**, 085124 (2005).
[32] C. J. Umrigar, J. Toulouse, C. Filippi, S. Sorella, and R. G. Hennig, Phys. Rev. Lett. **98**, 110201 (2007).
[33] J. Toulouse and C. J. Umrigar, J. Chem. Phys. **126**, 084102 (2007).
[34] W. H. Press, S. A. Teukolsky, W. T. Vetterling, and B. P. Flannery, *Numerical Recipes* (Cambridge University Press, Cambridge, U.K., 2002).
[35] R. J. Needs, M. D. Towler, N. D. Drummond, and P. López Ríos, computer code CASINO2.0 (University of Cambridge, Cambridge, 2006).
[36] L. Klynning and B. Lindgren, Ark. Fys. **32**, 575 (1966).
[37] M. D. Brown, J. R. Trail, P. López Ríos, and R. J. Needs, J. Chem. Phys. **126**, 224110 (2007).
[38] M. Casula, C. Attaccalite, and S. Sorella, J. Chem. Phys. **121**, 7110 (2004).
[39] M. Bajdich, L. Mitas, G. Drobný, L. K. Wagner, and K. E. Schmidt, Phys. Rev. Lett. **96**, 130201 (2006).
[40] P. López Ríos, A. Ma, N. D. Drummond, M. D. Towler, and R. J. Needs, Phys. Rev. E **74**, 066701 (2006).
[41] N. D. Drummond and R. J. Needs, J. Chem. Phys. **124**, 224104 (2006).
[42] E. L. Shirley and R. M. Martin, Phys. Rev. B **47**, 15413 (1993).
[43] Y. Lee and R. J. Needs, Phys. Rev. B **67**, 035121 (2003).
[44] R. Maezono, M. D. Towler, Y. Lee, and R. J. Needs, Phys. Rev. B **68**, 165103 (2003).
[45] X. Xu and W. A. Goddard, J. Chem. Phys. **121**, 4068 (2004).
[46] B. K. Lee, J. M. Stout, and C. E. Dykstra, J. Mol. Struct.: THEOCHEM **400**, 57 (1997).
[47] M. W. Lee, M. Mella, and A. Rappe, J. Chem. Phys. **122**, 244103 (2005).
[48] http://www.tcm.phy.cam.ac.uk/~mdt26/casino2_pseudopotentials.html